Journal of Zhejiang University SCIENCE A
ISSN 1673-565X (Print); ISSN 1862-1775 (Online)
www.zju.edu.cn/jzus; www.springerlink.com
E-mail: jzus@zju.edu.cn

A novel posture alignment system for aircraft wing assembly

Bin ZHANG[†], Bao-guo YAO[†‡], Ying-lin KE

(*College of Mechanical and Energy Engineering, Zhejiang University, Hangzhou 310027, China*)

[†]E-mail: zhwwbin@163.com; yaobg@zju.edu.cn

Received Feb. 23, 2009; Revision accepted May 31, 2009; Crosschecked Sept. 7, 2009

Abstract: A novel 6-degree of freedom (DOF) posture alignment system, based on 3-DOF positioners, is presented for the assembly of aircraft wings. Each positioner is connected with the wing through a rotational and adsorptive half-ball shaped end-effector, and the positioners together with the wing are considered as a 3-PPPS (P denotes a prismatic joint and S denotes a spherical joint) redundantly actuated parallel mechanism. The kinematic model of this system is established and a trajectory planning method is introduced. A complete analysis of inverse dynamics is carried out with the Newton-Euler algorithm, which is used to find the desired actuating torque in the design and path planning phase. Simulation analysis of the displacement and actuating torque of each joint of the positioners based on inverse kinematics and dynamics is conducted, and the results show that the system is feasible for the posture alignment of aircraft wings.

Key words: Aircraft wings, Three-coordinate positioner, Posture alignment, Kinematics, Dynamics
doi:10.1631/jzus.A0820777 **Document code:** A **CLC number:** V262.4

INTRODUCTION

During the conventional assembly of airplanes, fixtures specially designed according to the geometry of the structures are used to position and align the subassemblies. These fixtures are actuated with multiple mechanical actuators, which are sequentially driven by such means as hand cranks or pneumatic motors to achieve the desired motions. Since the actuators in these traditional systems are independent devices, the movement of the actuators cannot be truly coordinated and the fixtures may move along complex paths. Therefore, the assembly motion is inaccurate and unpredictable. In addition, the actuators can potentially counteract each other, thus imparting unwanted forces to the aircraft structures.

To solve these problems, a novel posture alignment system for use in the posture alignment of aircraft wings, is presented. In this new system, the wing is positioned and aligned with three three-coordinate positioners. Each positioner is attached to the wing with a rotational and adsorptive half-ball shaped end-effector. Posture of the wing is measured using a laser-tracking system and the trajectory of each positioner is preplanned. The wing can be controlled to move in any of three linear or three rotational paths. According to the theory of the mechanism, the combination of all the positioners and the wing can be considered as a 3-PPPS (P denotes a prismatic joint and S denotes a spherical joint) redundantly actuated parallel mechanism. Like other parallel mechanisms (Kim *et al*., 2001; Pietsch *et al*., 2005; Zuo *et al*., 2006), the alignment system performs well in comparison with serial mechanisms in terms of accuracy, rigidity, and its ability to handle large objects. Also, the attribute of actuating redundancy can yield an optimal load distribution (Cheng *et al*., 2001) among the actuators. Thus, actuator singularity can be avoided and the output force can be more homogenous and symmetric (Xia *et al*., 2004). Additionally, preload can be controlled to prevent backlash during motion (Müller, 2005).

The kinematic and dynamic models of the alignment system are established in this paper, and the trajectory planning method is discussed.

[‡]Corresponding author

MECHANICAL ARCHITECTURE

The aircraft wing to be aligned is supported by three three-coordinate positioners (Fig.1). The supported positions are the structural parts of the wing, such as ribs, spars or stringers. Each positioner has 5 parts: an *x*-axis slide block, a *y*-axis slide block, a cylinder, a *z*-axis telescopic rod and an end-effector. The rod moves along the axis of the cylinder, which is fixed on the *y*-axis slide block. The end-effector mounted on the top of the rod is used to connect the positioner to the skin of the wing.

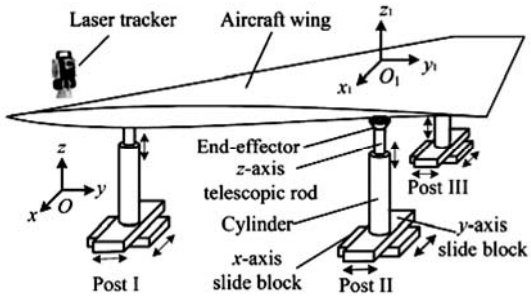

Fig.1 Schematic diagram of the posture alignment system

All of the actuating joints (*x*, *y* slide blocks and *z*-axis telescopic rod) are driven by servo motors. The couplings and ball screws are mounted on these axes to transmit the actuating torque. There is an additional retarder on the *z*-axis. Positions of these joints are measured and fed back by grating sensors.

A 3D model of the end-effector is shown in Fig.2. It consists of a vacuum cupule, a nylon ring, a half ball and a base. The vacuum cupule mounted on the half ball is made of rubber and is used to adsorb the wing skin. The half ball rotates in the cavity of the base, and the nylon ring is fixed on the edge of the ball to avoid scratch when aligning as its hardness is much lower than that of the aluminous alloy skin of the wing. Also, the ring is wearable and can provide sufficient static than that of the aluminous alloy skin of the wing. Also, the ring is wearable and can provide sufficient static friction force to prevent the end-effector from sliding on the skin of the wing.

Fig.2 3D model of the end-effector

The positioners together with the wing can be considered as a 6-DOF 3-PPPS parallel mechanism (Fig.3). The end-effectors act as spherical joints to connect the positioners to the wing. As the total number of the actuating joints is nine, which is more than the freedom of the system, the posture alignment system is redundantly actuated.

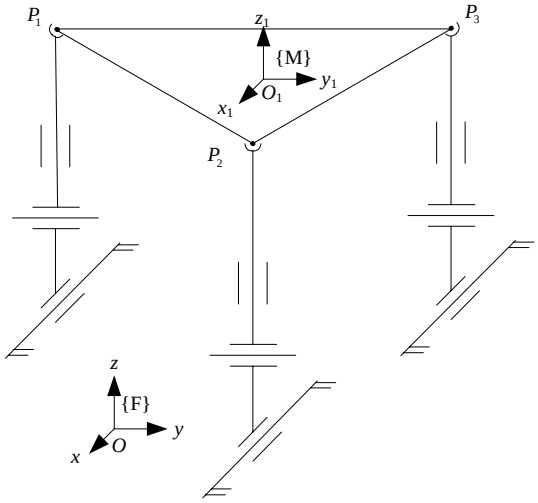

Fig.3 Kinematic structure of the system

P_1, P_2, P_3 are the centers of the end-effectors, {F} is the fixed coordinate, {M} is the moving coordinate

KINEMATIC ANALYSIS

Two coordinate frames are defined for the kinematic analysis of the alignment system. The first coordinate frame {F}: *Oxyz* is attached to the fixed base. The second coordinate frame {M}: $O_1x_1y_1z_1$ is attached to the aircraft wing. No errors are taken into account when modeling the kinematics.

Define the posture vector of the wing with respect to the frame {F} as

$$\boldsymbol{U} = \left[p_x, p_y, p_z, \phi, \theta, \psi \right]^{\mathrm{T}}, \tag{1}$$

where p_x, p_y, p_z denote the position of the origin point of the frame {M} and Φ, θ, ψ (Euler angles in the

sequence 313) denote the orientation of the frame {M} with respect to the frame {F}.

Denote the endpoint of the *i*th positioner (center of the end-effector) as $\boldsymbol{P}_i$ (*i*=1, 2, 3). Position vector of $\boldsymbol{P}_i$ can be defined as

$$\boldsymbol{q}_i = [q_{i1},\ q_{i2},\ q_{i3}]^{\mathrm{T}} \tag{2}$$

in the frame {F} and as

$$\boldsymbol{r}_i = [r_{i1},\ r_{i2},\ r_{i3}]^{\mathrm{T}} \tag{3}$$

in the frame {M}, where $\boldsymbol{r}_i$ is constant after the wing is located.

The rotation matrix of the frame {M} with respect to the frame {F} can be derived as

$$\boldsymbol{R} = \begin{bmatrix} \mathrm{c}\psi\,\mathrm{c}\varphi - \mathrm{s}\psi c\theta\,\mathrm{s}\varphi & -\mathrm{c}\psi\,\mathrm{s}\varphi - \mathrm{s}\psi\,\mathrm{c}\theta\,\mathrm{c}\varphi & \mathrm{s}\psi\,\mathrm{s}\theta \\ \mathrm{s}\psi\,\mathrm{c}\varphi + \mathrm{c}\psi\,\mathrm{c}\theta\,\mathrm{s}\varphi & -\mathrm{s}\psi\,\mathrm{s}\varphi + \mathrm{c}\psi\,\mathrm{c}\theta\,\mathrm{c}\varphi & -\mathrm{c}\psi\,\mathrm{s}\theta \\ \mathrm{s}\theta\,\mathrm{s}\varphi & \mathrm{s}\theta\,\mathrm{c}\varphi & \mathrm{c}\theta \end{bmatrix},$$

where c()≡cos() and s()≡sin().

The relationship between $\boldsymbol{q}_i$ and $\boldsymbol{r}_i$ is given as

$$\boldsymbol{q}_i = \boldsymbol{R}\boldsymbol{r}_i + \boldsymbol{X}, \tag{4}$$

where $\boldsymbol{X} = \left[p_x, p_y, p_z\right]^{\mathrm{T}}$.

By differentiating Eq.(4), the velocity vector of $\boldsymbol{P}_i$ can be derived as

$$\dot{\boldsymbol{q}}_i = \dot{\boldsymbol{R}}\boldsymbol{r}_i + \dot{\boldsymbol{X}}. \tag{5}$$

Eq.(5) can be rewritten as the form

$$\dot{\boldsymbol{U}} = \boldsymbol{J}\dot{\boldsymbol{q}}, \tag{6}$$

where $\dot{\boldsymbol{q}} = \left[\dot{\boldsymbol{q}}_1^{\mathrm{T}},\ \dot{\boldsymbol{q}}_2^{\mathrm{T}},\ \dot{\boldsymbol{q}}_3^{\mathrm{T}}\right]^{\mathrm{T}}$ denotes the velocity vector in the joint space, $\dot{\boldsymbol{U}}$ denotes the velocity vector in the task space, and $\boldsymbol{J}$ is the Jacobian matrix.

Continuing the differentiation of Eq.(5) gives the acceleration vector of $\boldsymbol{P}_i$:

$$\ddot{\boldsymbol{q}}_i = \ddot{\boldsymbol{R}}\boldsymbol{r}_i + \ddot{\boldsymbol{X}}. \tag{7}$$

Eqs.(4)~(7) are the basic kinematic equations of the posture alignment system.

TRAJECTORY PLANNING

Trajectory planning is used to find the appropriate displacement of each actuating joint so that the positioners can achieve the alignment motion synchronously. The posture of the wing during alignment is a function of time, which can be defined as $\boldsymbol{U}(t)$. Denote the initial and final postures as $\boldsymbol{U}_0$ and $\boldsymbol{U}_{\mathrm{tf}}$ respectively, and denote the duration of the alignment as t_{f}. To implement a continuous movement, $\boldsymbol{U}(t)$ must be subjected to the positional boundary constraints, shown as

$$\boldsymbol{U}(0) = \boldsymbol{U}_0, \tag{8}$$

$$\boldsymbol{U}(t_{\mathrm{f}}) = \boldsymbol{U}_{\mathrm{tf}}. \tag{9}$$

Also, to make the movement more smooth and stable, $\boldsymbol{U}(t)$ should be subjected to another two kinds of boundary constraints: velocity constraints described as

$$\dot{\boldsymbol{U}}(0) = 0, \tag{10}$$

$$\dot{\boldsymbol{U}}(t_{\mathrm{f}}) = 0, \tag{11}$$

and acceleration constraints described as

$$\ddot{\boldsymbol{U}}(0) = 0, \tag{12}$$

$$\ddot{\boldsymbol{U}}(t_{\mathrm{f}}) = 0. \tag{13}$$

Various kinds of functions, such as B-spline, polynomial, geodesic (Zefran *et al.*, 1998) and arc-length parameterized function (Saeed and Amir, 2006), have been used to express moving trajectories. To make it easier, a 5th order polynomial function is applied here as it can determine $\boldsymbol{U}(t)$ uniquely according to the constraint Eqs.(8)~(13).

By solving the equations above, $\boldsymbol{U}(t)$ can be derived as

$$\boldsymbol{U}(t) = \frac{6\Delta\boldsymbol{U}}{t_{\mathrm{f}}^5}t^5 - \frac{15\Delta\boldsymbol{U}}{t_{\mathrm{f}}^4}t^4 + \frac{10\Delta\boldsymbol{U}}{t_{\mathrm{f}}^3}t^3 + \boldsymbol{U}_0, \tag{14}$$

where $\Delta\boldsymbol{U}=\boldsymbol{U}_{\mathrm{tf}}-\boldsymbol{U}_0$ is the posture variety of the wing during the alignment.

Assuming that the initial position of $\boldsymbol{P}_i$ in the frame {F} is $\boldsymbol{q}_{i0}$, then, its position in the frame {M}

can be derived from Eq.(4) as

$$\boldsymbol{r}_{i0} = \boldsymbol{R}_0^{\mathrm{T}}(\boldsymbol{q}_{i0} - \boldsymbol{X}_0), \tag{15}$$

where $\boldsymbol{R}_0$ denotes the rotation matrix and $\boldsymbol{X}_0$ denotes the position vector of the wing at the time t=0. Since $\boldsymbol{r}_{i0}$ is constant during the alignment, the position of $\boldsymbol{P}_i$ in the frame {F} at any time can be obtained as

$$\begin{aligned}\boldsymbol{q}_i(t) &= \boldsymbol{R}(t)\boldsymbol{r}_{i0} + \boldsymbol{X}(t)\\ &= \boldsymbol{R}(t)\boldsymbol{R}_0^{\mathrm{T}}(\boldsymbol{q}_{i0} - \boldsymbol{X}_0) + \boldsymbol{X}(t),\end{aligned} \tag{16}$$

where $\boldsymbol{R}(t)$ is the rotation matrix and $\boldsymbol{X}(t)$ the position vector corresponding to $\boldsymbol{U}(t)$.

Denote the displacement of $\boldsymbol{P}_i$ as $\boldsymbol{S}_i$=[S_{i1}, S_{i2}, S_{i3}]$^{\mathrm{T}}$ which can be derived as

$$\begin{aligned}\boldsymbol{S}_i(t) &= \boldsymbol{q}_i(t) - \boldsymbol{q}_{i0}\\ &= \boldsymbol{R}(t)\boldsymbol{R}_0^{\mathrm{T}}(\boldsymbol{q}_{i0} - \boldsymbol{X}_0) + \boldsymbol{X}(t) - \boldsymbol{q}_{i0}.\end{aligned} \tag{17}$$

Because the actuating joints of each positioner move along their respective coordinate axes, each item of $\boldsymbol{S}_i(t)$ represents the trajectory of each actuating joint. From Eq.(17) we can find that $\boldsymbol{S}_i(t)$ is completely determined by $\boldsymbol{U}(t)$, which is predetermined by Eq.(14). So the trajectory of each actuating joint can be acquired through Eq.(17). The desired trajectory of each actuating joint can be tracked by a joint space PID (proportion, integral, derivative) controller (Cheng *et al*., 2001).

DYNAMIC ANALYSIS

To obtain the desired actuating torque, which is used to choose the model of motors and to design the mechanical system to ensure feasibility of the system in the design and path planning phase, the inverse dynamics of the alignment system are analyzed.

Lagrange-D'Alembert formulations (Cheng *et al.*, 2003) and the Newton-Euler algorithm (Kim *et al*., 2006) are the methods commonly used for dynamic modeling. The Newton-Euler algorithm is used here to establish the dynamics of the alignment system.

Dynamics of the wing

According to the Newton-Euler algorithm, the dynamic equations of the wing can be written in the following form:

$$\begin{cases} m_{\mathrm{B}}(\ddot{\boldsymbol{X}} - \boldsymbol{g}) = \sum_{i=1}^{3} \boldsymbol{R}\boldsymbol{f}_i, \\ \boldsymbol{I}_{\mathrm{B}}\dot{\boldsymbol{\omega}} + \tilde{\boldsymbol{\omega}}\boldsymbol{I}_{\mathrm{B}}\boldsymbol{\omega} = \sum_{i=1}^{3} \tilde{\boldsymbol{r}}_i \boldsymbol{f}_i, \end{cases} \tag{18}$$

where m_{B} is the mass of the wing, $\boldsymbol{I}_{\mathrm{B}}$ is the inertia matrix about the frame {M}, $\boldsymbol{\omega}$ is the angular velocity about the frame {M}, $\boldsymbol{f}_i$ is the force applied on the wing by the ith positioner and described in the frame {M}, $\boldsymbol{g}$ is the gravity vector, and $\tilde{\boldsymbol{\omega}}$ and $\tilde{\boldsymbol{r}}_i$ are the skew-symmetric matrixes of $\boldsymbol{\omega}$ and $\boldsymbol{r}_i$ respectively.

The angular velocity $\boldsymbol{\omega}$ is determined by the Euler angles via

$$\boldsymbol{\omega} = \begin{bmatrix} \dot{\psi}\,\mathrm{s}\theta\,\mathrm{s}\varphi + \dot{\theta}\,\mathrm{c}\varphi \\ \dot{\psi}\,\mathrm{s}\theta\,\mathrm{c}\varphi - \dot{\theta}\,\mathrm{s}\varphi \\ \dot{\psi}\,\mathrm{c}\theta + \dot{\varphi} \end{bmatrix}, \tag{19}$$

and the angular acceleration $\dot{\boldsymbol{\omega}}$ is expressed as

$$\dot{\boldsymbol{\omega}} = \begin{bmatrix} \ddot{\psi}\,\mathrm{s}\theta\,\mathrm{s}\varphi + \dot{\psi}\dot{\theta}\,\mathrm{c}\theta\,\mathrm{s}\varphi + \dot{\psi}\dot{\varphi}\,\mathrm{s}\theta\,\mathrm{c}\varphi + \ddot{\theta}\,\mathrm{c}\varphi - \dot{\theta}\dot{\varphi}\,\mathrm{s}\varphi \\ \ddot{\psi}\,\mathrm{s}\theta\,\mathrm{c}\varphi + \dot{\psi}\dot{\theta}\,\mathrm{c}\theta\,\mathrm{c}\varphi - \dot{\psi}\dot{\varphi}\,\mathrm{s}\theta\,\mathrm{s}\varphi - \ddot{\theta}\,\mathrm{s}\varphi - \dot{\theta}\dot{\varphi}\,\mathrm{c}\varphi \\ \ddot{\psi}\,\mathrm{c}\theta - \dot{\psi}\dot{\theta}\,\mathrm{s}\theta + \ddot{\varphi} \end{bmatrix}. \tag{20}$$

Dynamics of the *i*th positioner

Define the actuating torque vector of the ith positioner as

$$\boldsymbol{\tau}_i = \left[\tau_{i1}, \tau_{i2}, \tau_{i3}\right]^{\mathrm{T}}, \tag{21}$$

where τ_{i1}, τ_{i2} and τ_{i3} are the actuating torques on the x-, y-, and z-axes respectively. Parameters of the system are given in Table 1.

The actuating torque of the ith positioner can be derived as

$$\begin{aligned}\boldsymbol{\tau}_i = \boldsymbol{E}[&\boldsymbol{M}_1\ddot{\boldsymbol{q}}_i + \boldsymbol{R}\boldsymbol{f}_i\\ &+ \boldsymbol{D}_i\boldsymbol{\mu}(\boldsymbol{M}_2\boldsymbol{g} + \boldsymbol{\zeta}\boldsymbol{R}\boldsymbol{f}_i + \boldsymbol{N}) - m_3\boldsymbol{g}] + \boldsymbol{T}_i,\end{aligned} \tag{22}$$

where

$$\boldsymbol{E}=\mathrm{diag}\left\{\frac{l}{2\pi},\frac{l}{2\pi},\frac{l\eta}{2\pi}\right\},$$

$$\boldsymbol{M}_1=\mathrm{diag}\{m_1+m_2+m_3,m_2+m_3,m_3\},$$

$$\boldsymbol{M}_2=\begin{bmatrix}0&0&m_1+m_2+m_3\\0&0&m_2+m_3\\0&0&0\end{bmatrix},$$

$$\boldsymbol{N}=\left[m_3\ddot{q}_{i3},m_3\ddot{q}_{i3},0\right]^{\mathrm{T}},$$

$$\boldsymbol{\zeta}=\begin{bmatrix}0&0&1\\0&0&1\\0&0&0\end{bmatrix},$$

$$\boldsymbol{D}_i=\mathrm{diag}\{\mathrm{sign}(\dot{q}_{i1}),\mathrm{sign}(\dot{q}_{i2}),0\},$$

$$\boldsymbol{\mu}=\mathrm{diag}\{\mu,\mu,0\},$$

$$\boldsymbol{T}_i=\left[\frac{J_1 2\pi}{l}\ddot{q}_{i1},\frac{J_2 2\pi}{l}\ddot{q}_{i2},\frac{J_3 2\pi}{\eta l}\ddot{q}_{i3}\right]^{\mathrm{T}}.$$

Table 1 Parameters of the positioner

Parameter	Value
Mass of the *x*-axis slide block m_1 (kg)	110
Total mass of the *y*-axis slide block and the cylinder m_2 (kg)	250
Mass of the telescopic rod m_3 (kg)	35
Lead of the screws l (mm)	5
Speed reduce ratio of *z*-axis retarder η	0.02
Equivalent inertia of the screws J_1 (kg·mm^2)	5×10^{-5}
Equivalent inertia of the retarder J_2 (kg·mm^2)	5×10^{-5}
Equivalent inertia of the motors J_3 (kg·mm^2)	1×10^{-3}
Friction coefficient μ	0.02

Inverse dynamics solution

Eq.(18) can be rewritten as

$$\boldsymbol{P}=\boldsymbol{W}\boldsymbol{F}, \tag{23}$$

where

$$\boldsymbol{F}=\left[\boldsymbol{f}_1^{\mathrm{T}}\quad\boldsymbol{f}_2^{\mathrm{T}}\quad\boldsymbol{f}_3^{\mathrm{T}}\right]^{\mathrm{T}},$$

$$\boldsymbol{P}=\begin{bmatrix}m_{\mathrm{B}}\boldsymbol{R}^{\mathrm{T}}(\ddot{\boldsymbol{X}}-\boldsymbol{g})\\\boldsymbol{I}_{\mathrm{B}}\dot{\boldsymbol{\omega}}+\tilde{\boldsymbol{\omega}}\boldsymbol{I}_{\mathrm{B}}\boldsymbol{\omega}\end{bmatrix},$$

$$\boldsymbol{W}=\begin{bmatrix}\boldsymbol{I}_3&\boldsymbol{I}_3&\boldsymbol{I}_3\\\tilde{\boldsymbol{r}}_1&\tilde{\boldsymbol{r}}_2&\tilde{\boldsymbol{r}}_3\end{bmatrix}.$$

$\boldsymbol{I}_3$ is a 3×3 identity matrix.

Using the method of pseudoinverse matrix, the general solution of Eq.(23) can be derived as

$$\boldsymbol{F}=\boldsymbol{W}^{+}\boldsymbol{P}+(\boldsymbol{I}_9-\boldsymbol{W}^{+}\boldsymbol{W})\boldsymbol{\varepsilon}, \tag{24}$$

where $\boldsymbol{W}^{+}=(\boldsymbol{W}^{\mathrm{T}}\boldsymbol{W})^{-1}\boldsymbol{W}^{\mathrm{T}}$ is the Moore-Penrose pseudoinverse matrix of $\boldsymbol{W}$, $\boldsymbol{\varepsilon}$ is a 9×1 arbitrary matrix, and $\boldsymbol{I}_9$ is a 9×9 identity matrix. The first item contains mainly the actuating forces required for the alignment, and the second item is used for generating the inner forces of the wing. Since the inner forces are much smaller than the actuating forces during the alignment, we have the approximate solution with $\boldsymbol{\varepsilon}$=0, which minimizes $\boldsymbol{F}^{\mathrm{T}}\boldsymbol{F}$ and can be written as

$$\boldsymbol{F}=\boldsymbol{W}^{+}\boldsymbol{P}. \tag{25}$$

Substitution of Eq.(25) in Eq.(22) yields

$$\begin{aligned}\boldsymbol{\tau}_i=&\boldsymbol{E}[(\boldsymbol{I}_3+\boldsymbol{D}_i\boldsymbol{\mu}\boldsymbol{\zeta})\boldsymbol{R}\boldsymbol{K}_i\boldsymbol{W}^{+}\boldsymbol{P}]\\&+\boldsymbol{E}[\boldsymbol{M}_1\ddot{\boldsymbol{q}}_i+\boldsymbol{D}_i\boldsymbol{\mu}(\boldsymbol{M}_2\boldsymbol{g}+\boldsymbol{N})-m_3\boldsymbol{g}]+\boldsymbol{T}_i,\end{aligned} \tag{26}$$

where

$$\boldsymbol{K}_1=[\boldsymbol{I}_3,\ \boldsymbol{0},\ \boldsymbol{0}],$$

$$\boldsymbol{K}_2=[\boldsymbol{0},\ \boldsymbol{I}_3,\ \boldsymbol{0}],$$

$$\boldsymbol{K}_3=[\boldsymbol{0},\ \boldsymbol{0},\ \boldsymbol{I}_3].$$

SIMULATION

To show the kinematic and dynamic response of the system, a simulation analysis of the displacement and actuating torque of each joint of the positioners based on the inverse kinematics and dynamics was conducted using Matlab. The simulation parameters were assigned as follows:

$\boldsymbol{U}_0$=[50, 60, −35, 0.025, −0.022, 0.005]$^{\mathrm{T}}$;
$\boldsymbol{U}_{\mathrm{tf}}$=[0, 0, 0, 0, 0, 0]$^{\mathrm{T}}$;
$\boldsymbol{r}_1$=[500, 1100, 1200]$^{\mathrm{T}}$;
$\boldsymbol{r}_2$=[−450, 1320, 1250]$^{\mathrm{T}}$;
$\boldsymbol{r}_3$=[250, −1500, 1100]$^{\mathrm{T}}$;
m_{B}=500 kg;
$\boldsymbol{I}_{\mathrm{B}}$=diag{780 N·m^2, 750 N·m^2, 830 N·m^2};
t_{f}=20 s.

The simulation results for displacement of each actuating joint are shown in Fig.4. Fig.5 shows the simulation results for the desired actuating torque of each joint.

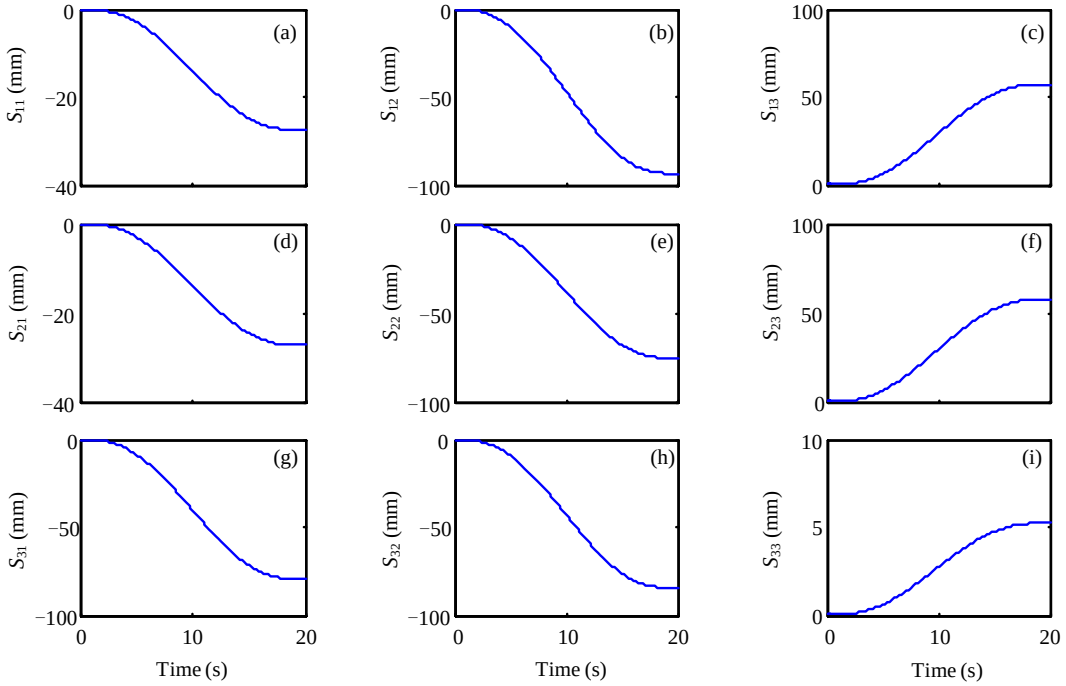

Fig.4 **Simulation results of the displacement of each actuating joint**

(a), (b), (c) are the results of positioner 1; (d), (e), (f) are the results of positioner 2; (g), (h), (i) are the results of positioner 3

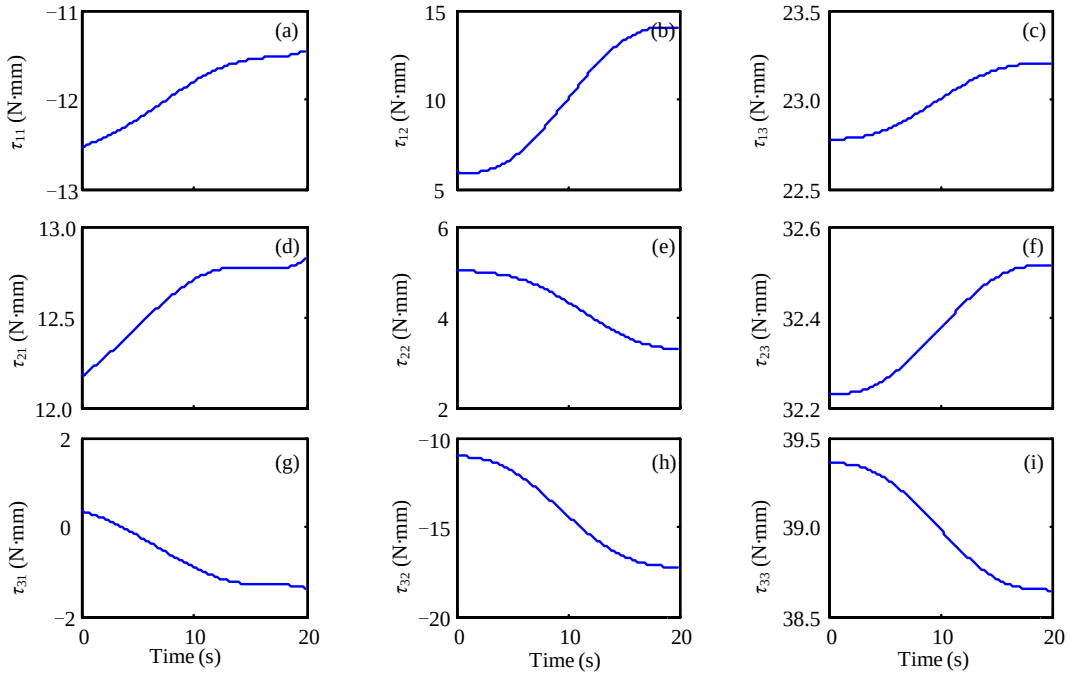

Fig.5 Desired actuating torque of each actuating joint

(a), (b), (c) are the results of positioner 1; (d), (e), (f) are the results of positioner 2; (g), (h), (i) are the results of positioner 3

The simulation results show that the displacement trajectories and the actuating torque of each joint of the positioners are continuous and smooth. Therefore, the trajectories can be accurately tracked by the PID controllers, and the posture alignment of the aircraft can be achieved.

CONCLUSION

A novel posture alignment system and method for aircraft wings was proposed. The kinematics, dynamics and trajectory planning of the system were discussed. The simulation results of the inverse kinematics and dynamics of the alignment system show that the system is feasible for the posture alignment of aircraft wings.

References

Cheng, H., Liu, G.F., Yiu, Y.K., Xiong, Z.H., Li, Z.X., 2001. Advantages and Dynamics of Parallel Manipulators with Redundant Actuation. International Conference on Intelligent Robots and Systems, USA, p.171-176.

Cheng, H., Yiu, Y.K., Li, Z.X., 2003. Dynamics and control of redundantly actuated parallel manipulators. *IEEE/ASME Transactions on Mechatronics*, **8**(4):483-491. [doi:10.1109/TMECH.2003.820006]

Kim, J., Park, F.C., Ryu, S.J., Kim, J., Hwang, J.C., Park, C., Iurascu, C.C., 2001. Design and analysis of a redundantly actuated parallel mechanism for rapid machining. *IEEE Transactions on Robotics and Automation*, **17**(4):423-434.

Kim, J.Y., Milos, R.P., James, K.M., 2006. Dynamic modeling and torque estimation of FES-assisted arm-free standing for paraplegics. *IEEE Transactions on Neural Systems and Rehabilitation Engineering*, **14**(1):46-54. [doi:10.1109/TNSRE.2006.870489]

Müller, A., 2005. Internal preload control of redundantly actuated parallel manipulators—its application to backlash avoiding control. *IEEE Transactions on Robotics*, **21**(4):668-677. [doi:10.1109/TRO.2004.842341]

Pietsch, I.T., Krefft, M., Becker, O.T., Bier, C.C., Hesselbach, J., 2005. How to reach the dynamic limits of parallel robots? An autonomous control approach. *IEEE Transactions on Automation Science and Engineering*, **2**(4):369-380. [doi:10.1109/TASE.2005.851600]

Saeed, B., Amir, K., 2006. Time-optimal trajectory planning in cable-based manipulators. *IEEE Transaction on Robotics*, **3**(22):559-563. [doi:10.1109/TRO.2006.870663]

Xia, Y.S., Wang, J., Fok, L.M., 2004. Grasping-force optimization for multifingered robotic hands using a recurrent neural network. *IEEE Transactions on Robotics and Automation*, **20**(3):549-554. [doi:10.1109/TRA.2004.824946]

Zefran, M., Kumar, V., Croke, C.B., 1998. On the generation of smooth three-dimensional rigid body motions. *IEEE Transaction on Robotics and Automation*, **14**(4):576-588. [doi:10.1109/70.704225]

Zuo, K.C., Xie, L.Y., Zhang, M., He, X.H., Yu, P., 2006. Error Modeling and Accuracy Analysis of a Novel 3-DOF Parallel Machine Tool. Proceeding of the 6th World Congress on Intelligent Control and Automation, China, p.8472-8476.